

Recrystallization of tungsten wire for fabrication of sharp and stable nanoprobe and field-emitter tips

M. Greiner and P. Kruse

Department of Chemistry, McMaster University, 1280 Main Street West, Hamilton, Ontario, L8S 4M1, Canada

(Received 18 November 2006; accepted 21 January 2007; published online 27 February 2007)

Atomically sharp tungsten tips made from single crystal tungsten wire are superior to those made from cold-drawn polycrystalline wire but are rarely used due to their high price. We have devised a method of obtaining highly crystalline tungsten wire by recrystallizing cold-drawn wire. The effect of various heat treatments on the wire microstructure was observed using scanning electron microscopy and x-ray diffraction. A dramatic difference in the shapes of tips etched from cold-drawn and recrystallized wires was observed using transmission electron microscopy. The described annealing process is an inexpensive alternative to using single crystal wires. © 2007 American Institute of Physics. [DOI: 10.1063/1.2670293]

Tungsten tips are commonly used as field emitters,^{1,2} nanoprobes,³ and scanning tunneling microscope (STM) probes.⁴ Cold-drawn, polycrystalline wire can be used to make tips; however, the atomic-scale structure of cold-drawn wire (CDW) tips is uncontrollable, with apexes that consist of multiple protrusions, which are structurally unstable.^{5,6} Atomically sharp tips that have a well-defined shape and are mechanically stable under regular operating conditions have been produced previously using single crystal tungsten wire.^{4,5,7-9} Unfortunately, since single crystal tungsten wire is roughly 10 000 times more expensive than cold-drawn wire, it has not been able to replace cold-drawn wire in common use.

The use of CDW tips is particularly prevalent among the STM community. In STM, multiple protrusions can cause image artifacts, where tunneling occurs through more than one protrusion at once. Studies using CDW tips have also shown evidence of tip instabilities under the forces experienced during STM imaging, in which the tunneling protrusion separates from the tip and attaches to the sample surface.^{6,7} This “jumping” behavior has not been noted when using single crystal wire (SCW) tips. The problems arising from the use of CDW tips make STM imaging a laborious process, with results that are not always easy to reproduce. We believe that both the shape and the stability problems of CDW tips arise from the extremely high defect concentrations in the grains of cold-drawn wires. Since single crystal tungsten wire is far too expensive for routine use, we aimed to reduce the defect concentration of cold-drawn wire by recrystallizing it prior to tip fabrication. Therefore our tips would be formed from pristine crystals.

Deformed metals can be recrystallized by a process known as annealing,¹⁰ which involves heating the metal to a sufficiently high temperature well below its melting point such that solid-state diffusion becomes appreciable. When a highly deformed, polycrystalline metal is annealed, its internal structure undergoes severe changes. Initially, the grains undergo recovery during which the point defect and dislocation densities are reduced. After recovery, recrystallization occurs in which new, pristine grains nucleate in highly de-

formed regions and grow, consuming the previous deformed grains. After recrystallization, a few grains continue to increase in size in a process called grain growth.¹¹

Annealing was accomplished by passing a high current through a 0.25 mm diameter, 13 cm long, 99.99% pure polycrystalline tungsten wire (Sigma-Aldrich) in vacuum ($P \sim 10^{-6}$ torr). The wire was mounted into a titanium sublimation pump (TSP) cartridge filament source (Varian, but any brand will do) in place of one of the titanium filaments. The TSP was then attached to a vacuum chamber, and the wire was resistively heated using an external dc power supply in constant current mode. A TSP power supply is not suitable for this purpose since it cannot provide the necessary voltage of up to 20 V. An ac voltage from a variable transformer could in principle be used, but the resistance of the tungsten wire changes significantly with temperature, requiring current rather than voltage regulation. Several dozen parameter combinations were tested. In order to optimize the annealing temperature, currents between 2.8 and 9.0 A were applied for times between 1 and 5 h (data not shown). Rapid recrystallization was observed for a current of 6.7 A (at approximately 14 V for our length wire). Using this current, annealing times of 10 s, 30 s, 1 min, 2 min, 5 min, 10 min, 30 min, and 1 h were tested (data in this article). One-quarter of the length of the wire was discarded at each end because it may not have reached the necessary annealing temperature due to cooling by the clamps. The temperature of the center part of the wires during annealing with 6.7 A was estimated to be around 1700 °C using an infrared pyrometer (Micron M90Q) through a view port on our test chamber. The pyrometer was calibrated up to 1200 °C using type K thermocouples attached to a tungsten wire, and the annealing temperatures of our samples were extrapolated from the calibration curve.

The structural changes caused by annealing were investigated using a scanning electron microscope (SEM). In order to make the microstructure more visible, the samples were electrochemically etched in a 3M NaOH solution using a platinum counterelectrode and applying a constant voltage

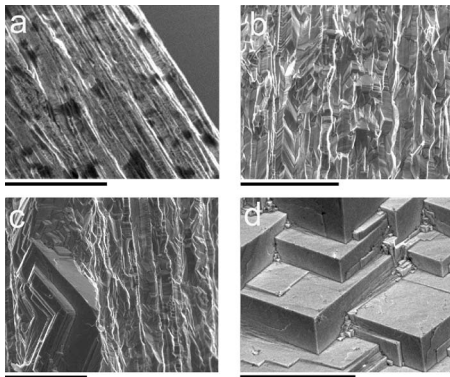


FIG. 1. SEM images showing grain structure of (a) nonannealed tungsten wire and wires annealed at 6.7 A for (b) 10 s, (c) 1 min, and (d) 30 min. All scale bars are 20 μm .

of 1.00 V for 15 min. The etching of a metal sample is commonly used in metallurgical analysis to highlight microstructural features.¹² Etching preferentially removes the least stable atoms, such as those surrounding defects and in certain crystal faces.¹³ Therefore polycrystalline and highly defected samples can be easily distinguished from pristine crystals. A highly defected grain will appear rough, while pristine grains will appear polyhedral, with sharp edges and flat faces containing numerous parallel step edges.

Some representative SEM images of etched wires from different annealing times are shown in Figs. 1(a)–1(d). For comparison, Fig. 1(a) shows a nonannealed wire. Its grains are long and fibrous, which is a result of the wire drawing process. The etched surfaces of the grains appear rough, due to the very high defect density, which results in a large number of small and poorly resolved etch features. Figure 1(b) shows a wire after an annealing time of 10 s. The grains have retained their fibrous shape; however, many parallel facets can now be seen within each grain. The fact that these facets can be resolved in the annealed wire indicates that the defect density of the grains has been reduced. This image is representative of the recovery stage of annealing.

The wire shown in Fig. 1(c) was annealed for about 1 min. In this image a newly formed crystallite can be distinguished from the deformed grain structure, indicating that after 1 min of annealing recrystallization had already begun. Note that while the new crystallite has a lower aspect ratio than the fibrous grains, it is slightly elongated, which indicates preferential grain growth along the wire axis. Figure 1(d) shows a wire after a 30 min annealing treatment. The original fiber texture is completely absent and is replaced by large crystallites.

X-ray diffraction (XRD) was used to confirm recrystallization. For comparison, diffraction data from a nonrecrystallized wire were obtained and compiled into a $\{110\}$ pole figure, as shown in Fig. 2(a). This pattern is typical of a cold-drawn bcc wire.¹⁴ There is a continuum of diffraction intensity, due to the essentially infinite number of orientations; however, the $[110]$ directions are preferentially aligned parallel with the wire axis. The reason for the preferential orientation is well understood and explained in Ref. 15.

A $\{110\}$ pole figure from a recrystallized wire is shown in Fig. 2(b). The sample used for this figure is the same as the one seen in Fig. 1(d). The pole figure shows sharp spots,

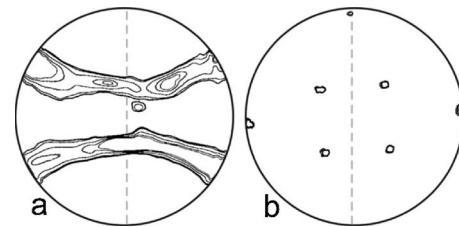


FIG. 2. X-ray diffraction data. Pole figures of $\{110\}$ reflections of (a) nonannealed wire and (b) wire annealed for 30 min at 6.7 A. The dashed lines indicate the wire axis.

with the correct angular relations and the requisite number of spots for $\{110\}$ planes of a bcc single crystal. Any additional spots in the pole figure would indicate polycrystallinity. Therefore we conclude that the x-ray beam was shining through one single crystal. Furthermore, since the beam diameter was 0.5 mm, and the wire diameter was 0.25 mm, we can conclude that the crystal under investigation spanned the whole diameter of the wire.

The orientation of the crystal in Fig. 2(b) with respect to the wire axis was determined. The $\langle 110 \rangle$ direction of the crystal is nearly parallel with the wire axis and is tilted by 3.5° in the $(1\bar{1}1)$ plane. Several other locations along the wire were investigated and also found to be single crystalline; however, the orientations differed from one to the next. The lengths of each crystalline domain ranged from 2 to 4 μm , in contrast to the cold-drawn grains observed by SEM, which were 1 μm in diameter and around 50 μm long.

Once recrystallization had been confirmed, tips were etched from the wire samples using the “lamellar drop-off” technique¹⁶ and the tip shapes were examined using a transmission electron microscope (TEM). Figure 3(a) shows an image of a tip made from a cold-drawn wire. This image shows multiple protrusions near the tip apex. The sample also shows nonuniform electron transmission, indicating variable sample thickness. Figure 3(b) is an image of a tip made from a fully recrystallized wire. The tip tapers off to a single protrusion and appears to be much more uniform, implying a more pristine lattice.

In conclusion, rapid recrystallization of 0.25 mm diameter, cold-drawn tungsten wire was achieved by resistive heating (6.7 A) in vacuum. Evidence of recrystallization was seen after only a few seconds of annealing. Primary recrystallization was typically complete after 30 min. X-ray diffraction measurements showed single crystalline regions spanning the entire wire diameter. Tips made from recrystallized wire were seen with TEM to have superior shapes to

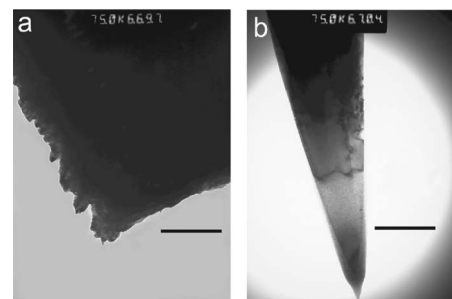


FIG. 3. TEM images of tips etched from (a) cold-drawn and (b) recrystallized wire. Scale bars are 250 nm.

tips made from cold-drawn wire. This recrystallization method is an inexpensive alternative to purchasing single crystal tungsten wire for use as field emitters or nanoprobe.

This project has been supported by funding from the Natural Sciences and Engineering Research Council of Canada. Constructive discussion with Dr. Marek Niewczas helped motivate the project. The authors also extend their appreciation to Jim Britten, Steve Kopprich, Andrew Duft, and Graham Pearson, for their valuable assistance.

- ¹J. Shi, Y. F. Lu, R. S. Cherukuri, K. K. Mendu, D. W. Doerr, D. R. Alexander, L. P. Li, and X. Y. Chen, *Appl. Phys. Lett.* **85**, 1009 (2004).
- ²H. S. Kuo, I. S. Hwang, T. Y. Fu, J. Y. Wu, C. C. Chang, and T. T. Tsong, *Nano Lett.* **4**, 2379 (2004).
- ³I. Shiraki, F. Tanabe, R. Hobaru, T. Nagao, and S. Hasegawa, *Surf. Sci.* **493**, 633 (2001).
- ⁴A. S. Lucier, M.S. thesis, McGill University, 2004.
- ⁵D. K. Biegelsen, F. A. Ponce, and J. C. Tramontana, *Appl. Phys. Lett.* **50**, 696 (1987).
- ⁶Y. Naitoh, K. Takayanagi, and M. Tomitori, *Surf. Sci.* **357–358**, 208 (1996).
- ⁷A. Schirmeisen, G. Cross, A. Stalder, P. Grütter, and U. Dürig, *Appl. Surf. Sci.* **157**, 274 (2000).
- ⁸P. Hoffrogge, H. Kopf, and R. Reichelt, *J. Appl. Phys.* **90**, 5322 (2001).
- ⁹H. W. Fink, *IBM J. Res. Dev.* **30**, 460 (1986).
- ¹⁰G. D. Rieck, *Acta Metall.* **6**, 360 (1958).
- ¹¹F. J. Humphreys and M. Hatherly, *Recrystallization and Related Annealing Phenomena*, 2nd ed. (Elsevier, Boston, 2004), p. 628.
- ¹²R. E. Smallman and R. J. Bishop, *Modern Physical Metallurgy and Materials Engineering*, 6th ed. (Butterworth-Heinemann, Oxford, 1999), Chap. 5.
- ¹³A. J. Melmed, *J. Vac. Sci. Technol. B* **9**, 601 (1991).
- ¹⁴S. K. Yerra, B. Verlinden, and P. Van Houtte, *Mater. Sci. Forum* **495–497**, 913 (2005).
- ¹⁵R. E. Smallman and R. J. Bishop, *Modern Physical Metallurgy and Materials Engineering*, 6th ed. (Butterworth-Heinemann, Oxford, 1999), Chap. 7.
- ¹⁶M. Klein and S. Schwitzgebel, *Rev. Sci. Instrum.* **68**, 3099 (1997).